Available online at www.sciencedirect.com

SciVerse ScienceDirect

Ceramics International 38 (2012) 6107–6113

CERAMICS INTERNATIONAL

www.elsevier.com/locate/ceramint

Phase transformation in tungsten carbide–cobalt composite during high temperature treatment in microwave hydrogen plasma

Alenka Vesel[a], Miran Mozetic[a], Marianne Balat-Pichelin[b,*]

[a]Jozef Stefan Institute, Jamova cesta 39, 1000 Ljubljana, Slovenia
[b]PROMES-CNRS Laboratory, 7 rue du Four Solaire, 66120 Font-Romeu Odeillo, France

Received 27 January 2012; received in revised form 13 April 2012; accepted 21 April 2012
Available online 3 May 2012

Abstract

To study phase formation up to 2300 K, tungsten carbide–cobalt (WC–Co) samples were exposed to concentrated solar radiation in hydrogen plasma. The reducing atmosphere was a non-equilibrium hydrogen plasma created in a microwave cavity at the nominal power of 1000 W. The dissociation fraction of hydrogen molecules in plasma was of the order of 10% assuring for almost optimal reduction of any oxide that could be formed on the surface of samples due to the residual atmosphere. Micro-structural characterization was performed by XRD and AES depth profiling. The results showed the appearance of Co_6W_6C phase at the temperature of 1050 ± 50 K. This phase almost vanished at the temperature of 1300 ± 90 K and was replaced by the Co_3W_3C phase. This phase vanished at 1690 ± 150 K where only WC and Co peaks were detected by XRD. The AES depth profiles showed enrichment of the surface film with Co at elevated temperatures. At extremely high temperature of 2300 K, the Co vanished from the surface layer but remained in crystalline form in the bulk material. SEM imaging showed an evolution of the material crystallinity up to perfectly recognizable crystals of the dimension of approx. 1 μm at the maximum temperature. The results are explained by mobility of Co atoms, surface segregation and sublimation at very high temperature.

Keywords: A. Thermal and plasma treatment; B. Electron spectroscopy; D. Tungsten carbide; E. Refractories

1. Introduction

Tungsten carbide cobalt composite is extremely hard and has excellent wear resistance. Therefore it is widely used as protective coatings of cutting tools for machining, cutting, drilling of many materials [1]. The composition of this material allows for almost perfect mechanical properties. This material, as many other composites, may not be perfectly stable at elevated temperatures. Any changes in the structure as well as composition of the material may lead to a loss of the mechanical properties. Although this material is widely used, little work has been performed on the characterization of structural modifications and other effects which may appear due to heating of the material at elevated temperatures [1,2]. The aim of this paper is to detect and characterize any structural and compositional changes in a surface film of sub-micrometer thickness that may occur at elevated temperatures. Since we wanted to avoid any oxidation of the material during the thermal treatment and also during cooling of samples down to room temperature, we used hydrogen plasma as a protective atmosphere. Namely, hydrogen plasma is well known to be extremely reducing and is capable of immediate removal of any oxide that might form on a surface of materials at elevated temperatures [3–8].

2. Materials and experimental protocol

A sample of WC94/Co6 (25×25 mm^2) was supplied by Goodfellow. The sample was cut to small pieces of about 1 cm × 1 cm. The thickness of the sample was 2 mm. No surface finishing or cleaning was performed prior to experiments due to the well known fact that hydrogen plasma treatment allows for removal of traces of different impurities such as oxides and organic impurities [3–6].

*Corresponding author. Tel.: +33 468 307 768; fax: +33 468 302 940.
E-mail address: marianne.balat@promes.cnrs.fr (M. Balat-Pichelin).

0272-8842/$36.00 © 2012 Elsevier Ltd and Techna Group S.r.l. All rights reserved.
http://dx.doi.org/10.1016/j.ceramint.2012.04.058

Samples were exposed to highly non-equilibrium hydrogen plasma created in a quartz glass tube placed in the center of a microwave discharge. Schematic of the experimental system is shown in Fig. 1. The quartz tube is pumped with a two stage rotary pump with an ultimate pressure below 1 Pa and the nominal pumping speed of 33 $m^3 h^{-1}$. On the other side, hydrogen of purity 99.99% was leaked into the quartz tube through a mass flow controller. The flow rate was fixed at 12 l h^{-1}. Plasma was concentrated into the cavity volume around the sample as shown in Fig. 1. The inner diameter of the quartz tube was 5 cm and the plasma volume was about 110 cm^3. The nominal microwave power was set to 1000 W. At such conditions, the dissociation fraction of hydrogen plasma was of the order of 10% [9]. Such a large concentration of H atoms allows for immediate removal of any oxygen from the surface of a sample. Highly non-equilibrium state of plasma ensures for minimal heating of samples by plasma itself. The samples were heated rather by exposure to concentrated solar radiation [9,10] as shown schematically in Fig. 1.

The temperature of the samples during plasma treatment was monitored by a calibrated IR pyrometer. The pyrometer operates at the wavelength of 5 μm. The accuracy of the temperature is estimated to about 1000 ± 50 K, 1300 ± 90 K, 1600 ± 150 K and 2300 ± 190 K due to the accuracy on the spectral directional emissivity (0.25–0.30) taken for this material [11]. Samples were mounted into the system shown in Fig. 1. After evacuation down to the ultimate pressure, hydrogen was injected into the quartz tube with continuous pumping. The working pressure of 40 Pa was therefore established and kept at this value during the thermal treatment of any sample. The microwave generator was turned on, so hydrogen in the reactor transformed in the state of plasma. Hydrogen plasma

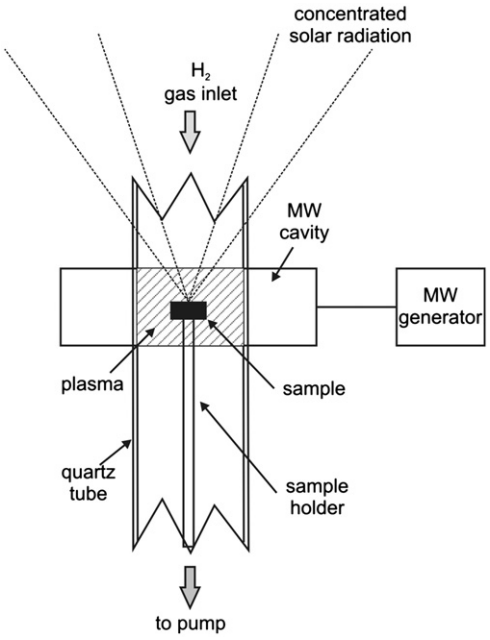

Fig. 1. Schematic of the experimental system.

created in our system is highly non-equilibrium meaning that its chemical reactivity is rather large taking into account the gas temperature which remains below say 500 K. Here, it is worth mentioning that the reactivity of hydrogen at equilibrium conditions may be comparatively large at elevated temperatures due to catalytic dissociation of hydrogen molecules on metallic surfaces. In our case, however, all surfaces facing plasma are supposed low-catalytic so this effect is minimized as long as no metal appears on the surface of the samples. The samples do not heat substantially by interaction with plasma particles (predominantly neutral H atoms in the ground state) but heating is realized by concentrated solar radiation as shown schematically in Fig. 1. The system thus allows for controlled and adjustable heating of samples independent from plasma parameters. As soon as a sample was exposed to concentrated solar radiation, its temperature rose well above the ambient one. In about 50 s, the sample temperature is stabilized at a value which depended on the solar flux. Since the solar flux is adjustable, any temperature up to about 2500 K is achievable. Samples were kept at selected temperatures for 250 s and after turning off the heating source, they slowly cooled down. When the temperature decreased below about 400 K, plasma source was turned off. Samples were not taken from the reactor before cooling down in order to prevent oxidation in air.

Before and after plasma treatment, the samples were characterized by X-ray diffraction (XRD), Auger electron spectroscopy depth profiling (AES) and scanning electron microscopy (SEM).

In order to reveal the crystalline nature of the surface we performed X-ray diffraction analysis. X-ray diffraction measurements were performed by using a Philips PW 1820 diffractometer equipped with a Cu Kα radiation source (1.5406 Å). The scanning region ranged from 15° to 75°, and the scanning rate was 0.02. AES depth profiling was performed using Scanning Auger Microprobe (Physical Electronics Ind. SAM 545 A). Samples were excited with a static primary electron beam with the energy of 3 keV, the beam current of 2 μA and the diameter of about 40 μm. The electron incidence angle with respect to the normal to the average surface plane was 30°. The samples were ion sputtered with two symmetrically inclined beams of 3 keV Ar^+ ions, rastered on a surface area larger than 5×5 mm^2 at an incidence angle of 47°. The sputtering rate as determined on a C/WC/W/Si multilayer standard was about 2.5 nm/min. Concentration profiles were evaluated by using relative sensitivity factors from the manufacturer's handbook. The Auger peak-to-peak heights of C (272 eV), O (510 eV), Co (775 eV) and W (179 eV) were measured. The following sensitivity factors were used: C (0.11), O (0.50), Co (0.27) and W (0.113).

The morphology of the samples was monitored by scanning electron microscopy. We used a high-resolution scanning electron microscopy FEG-SEM7600F from JEOL. Secondary electron images were taken at a magnitude of 10,000 × and at an accelerating voltage of 15 kV.

3. Experimental results

The evolution of X-ray diffraction patterns of WC–Co samples treated in hydrogen plasma at elevated temperatures is shown in Fig. 2. The lowest curve in Fig. 2 is for untreated (reference) sample. As expected, only peaks corresponding to tungsten carbide WC are detected. The corresponding data were taken from ICDD card 73-0471. Any cobalt peaks are below the detection limit. After annealing the sample to about 1050 ± 50 K (sample no. 1 in Fig. 2) new diffraction peaks appear indicating formation of Co_6W_6C (ICDD card 23-0939) with a small contribution of Co_3W_3C (ICDD card 27-1125). For the sample heated to about 1300 ± 90 K (sample no. 2 in Fig. 2) we can observe the opposite effect i.e. the intensity of the peaks due to Co_3W_3C is increased, while the intensity of the peaks due to Co_6W_6C is decreased. These peaks completely disappeared on the sample which was heated to about 1690 ± 150 K (sample no. 3 in Fig. 2). The diffraction peaks of tungsten carbide WC (indicated as WC in Fig. 2) almost vanish at 1300 K, but recover at 1690 K and remain predominant even at 2300 K. New small peaks appear at 1690 K and are attributed to crystalline cobalt Co (ICDD card 15-0806).

AES depth profiling is a complementary method to XRD. It shows surface composition of a sample but does not reveal the structure (crystallinity) of materials. The AES depth profiles of the samples treated at different temperatures are shown in Fig. 3. Fig. 3a is the depth

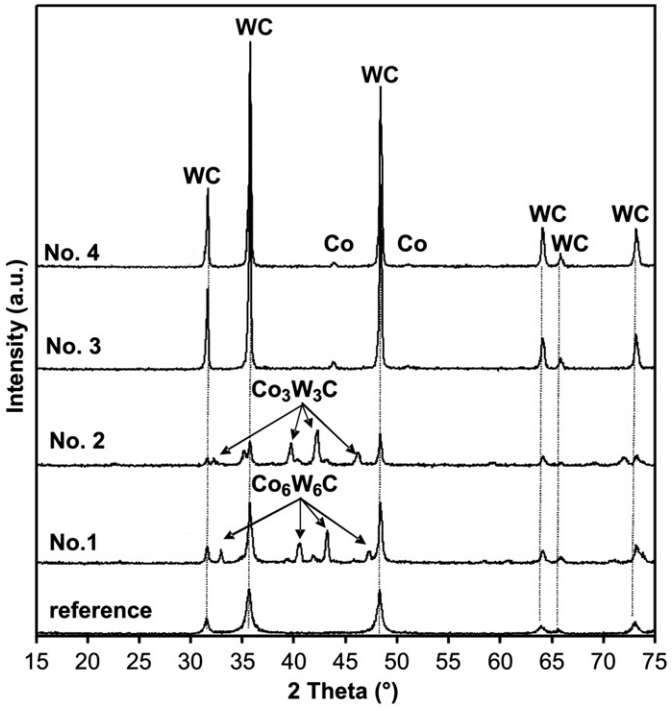

Fig. 2. X-ray diffraction patterns of plasma treated WC–Co samples at different temperatures: (reference) untreated sample, (no. 1) sample heated to 1050 ± 50 K, (no. 2) sample heated to 1300 ± 90 K, (no. 3) sample heated to 1690 ± 150 K and (no. 4) sample heated to 2300 ± 190 K.

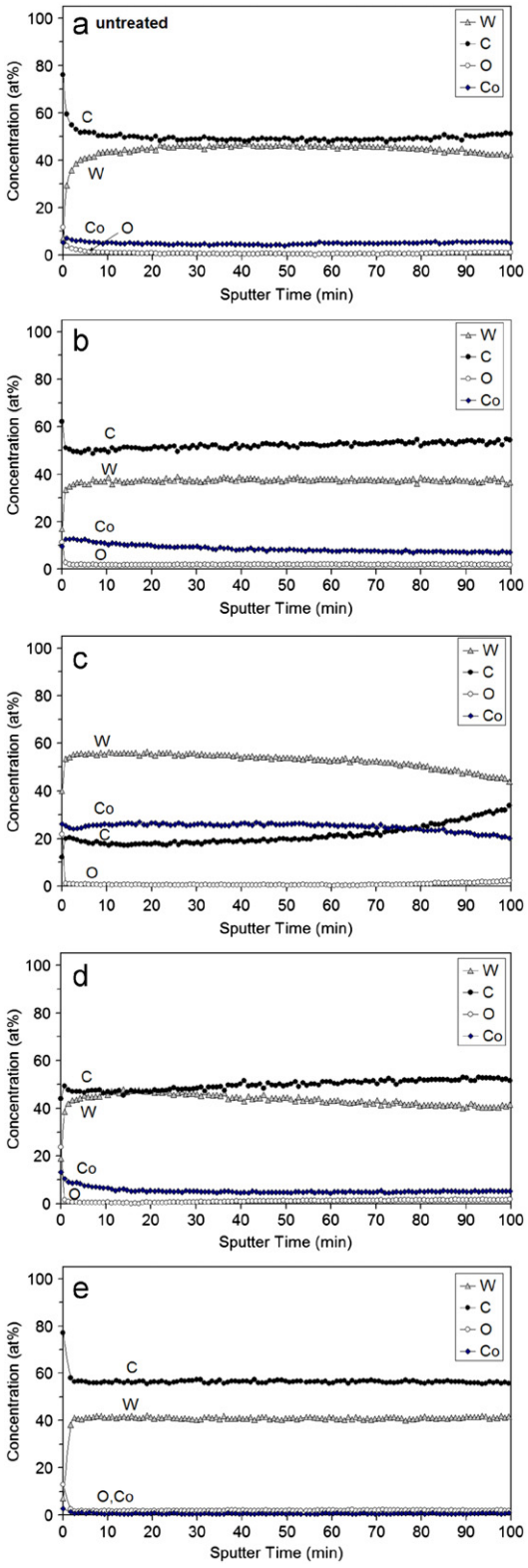

Fig. 3. AES depth profiles of (a) untreated sample, (b) sample heated to 1050 ± 50 K, (c) sample heated to 1300 ± 90 K, (d) sample heated to 1690 ± 150 K and (e) sample heated to 2300 ± 190 K.

profile of an untreated sample. As the sample is heated to 1050 K the depth profile remains similar to the untreated one except that the cobalt concentration is somehow enriched (Fig. 3b). The enrichment is most expressed in

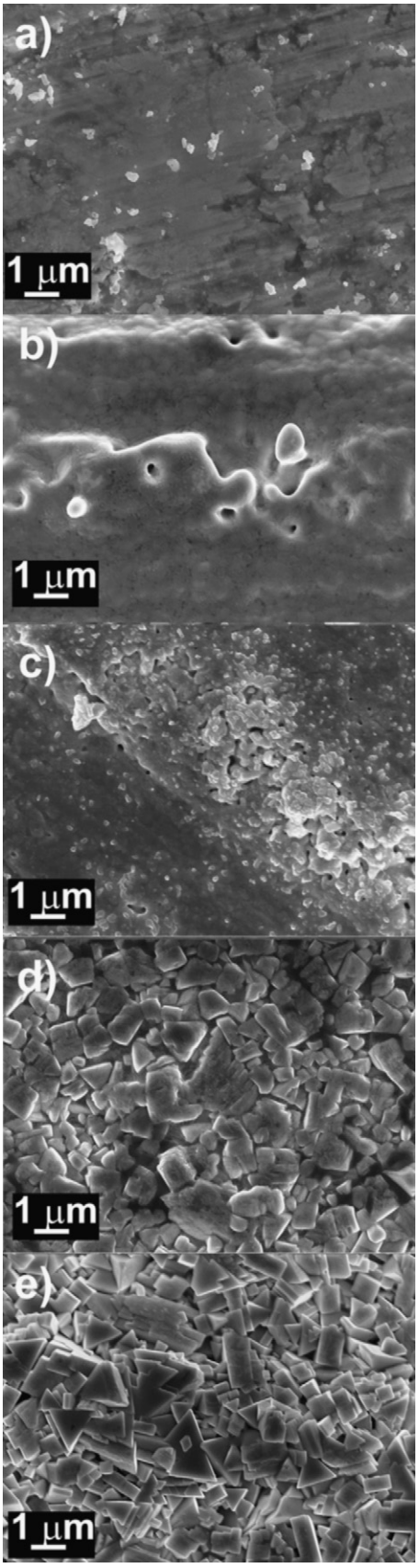

Fig. 4. SEM images of (a) untreated sample, (b) sample heated to 1050 ± 50 K, (c) sample heated to 1300 ± 90 K, (d) sample heated to 1690 ± 150 K and (e) sample heated to 2300 ± 190 K.

Fig. 3c which shows the depth profile at 1300 K. Further increase of temperature causes a decrease of the cobalt concentration in the surface film, while after treatment at 2300 K the cobalt concentration in the surface film of the sample falls below the detection limit of our AES device.

Scanning electron microscope images are shown in Fig. 4. Fig. 4a corresponds to the as-received sample. Treatment at 1050 K causes some modification of the surface morphology but no crystallites are observed (Fig. 4b). Fig. 4c was taken after the treatment at 1300 K and the surface morphology is much different from that observed for the untreated sample. Crystallites with the typical dimension of about 1 μm appear on the surface of the sample heated at 1690 K (Fig. 4d). These crystallites present almost perfect shape after heating at 2300 K as demonstrated in Fig. 4e.

4. Discussion

The results of thermal processing in hydrogen plasma reveal some interesting features and are worth discussing. Several different characterization techniques were used in order to be able to understand the evolution of the structural and compositional changes during sample treatment. Heating was performed in highly dissociated hydrogen plasma. Such an unusual medium was used in order to prevent any oxidation of the material. Namely, it is well known that metals oxidize at elevated temperatures even in protective atmosphere because traces of oxidizing impurities could never be avoided completely. Thin metal oxide films often represent a barrier for atom migration in thin films so it is recommended to avoid any oxidation in order to prevent such effects. Non-equilibrium hydrogen plasma thus allows for studying thermal effects in absence of effects caused by appearance of oxides. Oxidation itself, of course, cannot be avoided and it is well known that practically all metals (gold and alike) oxidize upon heating. The oxide, however, is removed by reactive hydrogen atoms immediately. Recently, we have shown that even relatively thick oxide films formed on stainless steel or tungsten are effectively reduced using highly reactive hydrogen plasma [4,5].

XRD characterization of the untreated sample (Fig. 2, the lowest curve) reveals only peaks that are attributed to tungsten carbide. The peaks are not extremely sharp. The width of the peaks could be easily attributed to the resolution of the spectrometer, but they could also be attributed to poor crystallinity. Namely, the uppermost curve in Fig. 2 exhibit much sharper peaks showing a better crystallinity. The AES depth profiling (Fig. 3a) cannot reveal the crystalline structure. It only reveals a very high concentration of carbon on the surface as well as oxygen. The high concentration of carbon is due to traces of impurities. As mentioned earlier no attempt was made to clean the material prior to experiments. Oxygen on the surface is probably just an extremely thin native film (contamination). SEM (Fig. 4a), on the other hand, may

reveal crystalline structure. From Fig. 4a we can just conclude that crystallites, if present, are smaller than the resolution of the SEM image.

As the sample is heated to 1050 ± 50 K, interesting modifications are observed by all three techniques. First, SEM shows an appearance of features with round shape on the surface of the sample (Fig. 4b). Second, AES depth profiling shows some enrichment of the cobalt content near the surface (Fig. 3b), and XRD shows new peaks that correspond to another phase Co_6W_6C. Obviously, cobalt which was originally diluted in the WC matrix interacts chemically with the matrix forming crystallites of this compound Co_6W_6C. Since the concentration of cobalt in the surface layer observed by AES is about 10 at% only, the Co_6W_6C crystallites are not very dense in the surface film so they cannot be distinguished from the SEM image presented in Fig. 4b.

Increasing the temperature to 1300 ± 90 K causes formation of interesting surface features, as shown in Fig. 4c. The SEM image does not reveal the composition of the features, but AES depth profiling (Fig. 3c) indicate that the features could probably be rich in cobalt. The XRD results (Fig. 2) clearly confirm this speculation. Namely, another crystalline structure is revealed by XRD and it corresponds to Co_3W_3C. Obviously, the increase of the temperature from 1050 to 1300 K causes a big change in the structure of the material, at least in the surface layer. It is interesting that the WC peaks almost vanish at 1300 ± 90 K. The rather low intensity of WC peaks in this XRD diffractogram however, does not necessarily mean that the entire sample has changed its structure. Namely, the penetration depth of X-rays is well below the thickness of our samples, so the only conclusion that can be drawn from the comparison of SEM, AES and XRD results is that the surface layer is enriched with Co_3W_3C phase on account of other phases.

The structure of the material heated to 1690 ± 150 K is completely different from previous ones. Not only that Co_6W_6C and Co_3W_3C phases have completely disappear, but very sharp WC peaks appear, and even a well pronounced Co peak becomes visible (Fig. 2). Interesting enough, the AES depth profile (Fig. 3d) shows an almost identical composition of the sample treated at 1690 K and the untreated sample. This observation clearly shows the limitations of the AES depth profiling. The corresponding SEM image is presented in Fig. 4d and reveals well defined crystallites at the surface of the material. The depletion of the surface layer as compared to the sample heated at 1300 K can be explained either by diffusion of cobalt back into the bulk or by surface segregation followed by sublimation. Since the quartz tube wall became dirty after this particular experiment and the AES characterization of the dirtiness reveals practically only cobalt, we can confirm the hypothesis of cobalt sublimation. The Co sublimation is obviously not complete as revealed by AES (Fig. 3d) and XRD (Fig. 2). The XRD results reveal that small crystals of pure cobalt are present in an almost perfect crystalline matrix.

Further heat treatment of the sample does not result in any structural changes as revealed from XRD measurements. The AES depth profiling, however, reveals that cobalt vanishes from the surface film (Fig. 3e). Obviously, the cobalt crystals that are observed by XRD are not found in the surface layer but are present in subsurface layer, definitely below the layer characterized by AES. SEM image of this sample (Fig. 4e) reveals perfect crystallites. Comparison of SEM image with AES and XRD confirms that the crystals observed in Fig. 4e are made from WC. Heating of the WC/Co samples to the very high temperature of 2300 K therefore recovers an almost perfect crystallinity of the WC phase on the surface of the samples. Here, it is worth mentioning that re-crystallization of solid materials often does not occur at temperatures well below the melting point. The melting point of tungsten carbide is at 3143 K. Almost perfect crystals observed on the surface of samples treated at highest temperature (Fig. 4e) could be explained either by the plasma effects or by underestimation of the sample temperature. It is known that plasma treatment may result in formation of almost ideal monocrystalline features on many samples [12,13] and this observation is not yet fully understood although an appropriate hypothesis has been launched recently [14]. The other possible explanation is inaccurate determination of the sample temperature. We did the best to calculate the right temperature from emission of the material measured by a calibrated pyrometer but since the normal spectral (at 5 μm) emissivity has not been determined for our particular sample but just taken from appropriate database [11] the temperature may be underestimated, this is why the given accuracy on each temperature level is so high.

At the end, it is worth to mention that formation of Co_3W_3C and Co_6W_6C is already known from literature [1,2]. It is also known that these two forms are not likely to coexist in the same WC–Co alloy as it is observed also in our case [2]. They may be transformed one into another with increasing temperature. It was reported that Co_3W_3C was detected at temperatures about 970 K by the reaction:

$$W + 3Co + C = Co_3W_3C$$

When temperature was increased to 1070 K, Co_3W_3C phase was transformed to Co_6W_6C phase by the following reaction:

$$2Co_3W_3C + W = Co_6W_6C + WC$$

This is in agreement with our experiment—in our case the minimum temperature was 1050 K and we have observed the formation of the Co_6W_6C phase. It is interesting that the authors of Ref. [2] have observed decomposition of Co_6W_6C into WC and Co when they have increased the temperature from 1070 to 1420 K. In our case, we have first observed the decomposition from Co_6W_6C to Co_3W_3C at temperature of about 1300 ± 90 K and then at 1690 ± 150 K we have observed the decomposition to WC and Co.

Interesting enough, our observations reported and discussed above as well observation of other authors [1,2] are different from results reported by Fang [15] and Milani [16] who both used thermodynamically almost perfectly equilibrium systems. Namely, the ternary phase diagram reveals a stable phase Co_6W_6C at temperatures below about 1420 K, and another stable phase Co_3W_3C above this temperature. The transition temperature under equilibrium conditions is therefore roughly at 1420 K. Our results, as well as results reported in [1,2] show much lower transition temperatures. As discussed above, the discrepancy could be attributed to wrong temperature estimation in our work as well as in work reported by [1,2]. On the other hand, the discrepancy may be due to the fact that the phase transitions in thin films occur at lower temperature than in bulk materials. Numerous authors have shown that the phase formation and disappearance in thin films and/or nanoscopic materials often appear at different temperatures than in bulk materials. Unfortunately we were not able to perform systematic experiments on bulk materials so both explanations could be used in order to interprete the results presented in this paper.

The concentration of carbon in the surface film was measured by AES. Although AES is not the most accurate technique for the determination of the absolute composition, big changes observed at different temperatures are worth discussing. The AES method determines the intensity of Auger electrons peaks and the concentration is determined using appropriate sensitivity factors. Care should be taken when using AES depth profiling in combination with ion sputtering. Namely, the sputtering could be preferential and it is well known that AES depth profiling of organic materials by sputtering with single argon ions is questionable. Heavier ions are recommended. In our case the materials are inorganic so selective removal by argon ion sputtering is less pronounced. Still, this effect definitely cannot explain the poor carbon concentration for the sample treated at 1300 K. A possible explanation could be enrichment of the surface layer by metal-rich phases—Co_3W_3C. Any comparison with XRD results is misleading since the information depths are not comparable. AES depth profile showed in Fig. 3c indicates that at this temperature the surface concentration of metals is the highest. An attentive observer will spot a small detail—at long sputtering time the carbon concentration increases and at 100 min (the longest sputtering time used) the concentration of carbon is already twice as high as in the thin film. Probably, longer sputtering times would reveal similar concentrations of carbon as in the other samples. The virtual discrepancy between AES and XRD results just indicate that the intensive phase formation occurs preferentially on the surface of the sample while the bulk remains less influenced.

5. Conclusion

Structural and compositional modifications in WC–Co composite during high-temperature treatment in highly non-equilibrium hydrogen plasma were observed by three complementary techniques: XRD, AES and SEM. The combination of these three techniques allowed for a rather good explanation of the behavior of this material at high temperature. The results can be summarized as follows: original samples contain tungsten carbide with not well expressed crystallinity degree and cobalt distributed evenly in the tungsten carbide matrix. As the samples are heated, cobalt starts reacting with WC forming the Co_6W_6C phase. This phase is rather stable at 1050 K but at higher temperatures it vanishes and is partially replaced by the Co_3W_3C phase. Simultaneously, migration of cobalt from the bulk towards the surface of the material is observed. With further increase of temperature, the Co_3W_3C phase becomes unstable, cobalt diffuses towards the surface of the sample and sublimates. At the temperature of 1690 K, cobalt practically segregates in the bulk forming crystallites. Even higher temperature does not cause substantial difference except that cobalt completely vanishes from the surface layer of the sample. All experiments were performed in highly reductive atmosphere and any oxidation of material was prevented. The results are therefore valid for pure system without any oxygen. The main role of plasma against ordinary heating of materials in protective atmosphere is summarized as the ability to reduce any oxides from the surface of treated materials as soon as they are formed. Otherwise, the thermal processing is not much different from classical heating so it is not surprising that all phases according to ternary diagrams were observed upon plasma treatment.

Acknowledgments

This project was funded by Slovenian Research Agency (ARRS) and through the Grant of the European FP7-SFERA program (2009–2013).

References

[1] K. Feng, J. Xiong, L. Sun, H. Fan, X. Zhou, The process of combustion synthesis of WC–Co composites under the action of an electric field, Journal of Alloys and Compounds 504 (2010) 277–283.
[2] Shun-hua Cao, Zhi-yong Cai, Zhou Jian-hua, Jiong-yi Li, Xin-ping Lin, Phase transformation of nano-grained W(Co, C) composite powder and its phase constitute, Journal of Central South University of Technology 13 (2006) 603–607.
[3] M. Mozetic, B. Pracek, Interaction of hydrogen plasma with corroded silver surface, Informacije MIDEM 28 (1998) 171–174.
[4] A. Vesel, A. Drenik, R. Zaplotnik, M. Mozetic, M. Balat-Pichelin, Reduction of thin oxide films on tungsten substrate with highly reactive cold hydrogen plasma, Surface and Interface Analysis 42 (2010) 1168–1171.
[5] M. Mozetic, A. Zalar, M. Drobnic, Reduction of thin oxide layer on $Fe_{60}Ni_{40}$ substrates in hydrogen plasmas, Thin Solid Films 343–344 (1999) 101–104.
[6] M. Mozetic, Discharge cleaning with hydrogen plasma, Vacuum 61 (2001) 367–371.
[7] T. Belmonte, J.M. Thiébaut, H. Michel, R.P. Cardoso, A. Maliska, Reduction of metallic oxides by late Ar–H_2–N_2 post-discharges. I. Application to copper oxides, Journal of Vacuum Science and Technology A 20 (2002) 1347–1352.

[8] T. Belmonte, J.M. Thiébaut, H. Michel, R.P. Cardoso, A. Maliska, Reduction of metallic oxides by late Ar–H_2–N_2 post-discharges. II. Applications to iron oxides, Journal of Vacuum Science and Technology A 20 (2002) 1353–1357.
[9] A. Vesel, A. Drenik, M. Mozetic, M. Balat-Pichelin, Hydrogen atom density in a solar plasma reactor, Vacuum 84 (2010) 969–974.
[10] A. Vesel, M. Mozetic, A. Drenik, N. Hauptman, M. Balat-Pichelin, High temperature oxidation of stainless steel AISI 316L in air plasma, Applied Surface Science 255 (2008) 1759–1765.
[11] Y.S. Touloukian, D.P. De Witt, Thermal radiative properties—non metallic solids, Thermophysical Properties of Matter TPRC Data Series, vol. 8, Plenum, New-York, 1972.
[12] U. Cvelbar, Z. Chen, M.K. Sunkara, M. Mozetic, Spontaneous growth of superstructure alpha-Fe_2O_3 nanowire and nanobelt arrays in reactive oxygen plasma, Small 4 (2008) 1610–1614.
[13] M. Mozetic, U. Cvelbar, A method for the rapid synthesis of large quantities of metal oxide nanowires at low temperatures, Advanced Materials 17 (2005) 2138–2142.
[14] K. Ostrikov, I. Levchenko, U. Cvelbar, M.K. Sunkara, M. Mozetic, From nucleation to nanowires: a single-step process in reactive plasmas, Nanoscale 2 (2010) 2012–2027.
[15] Z.Z. Fang, O.O. Eso, Liquid phase sintering of functionally graded WC–Co composities, Scripta Materialia 52 (2005) 785–791.
[16] R. Milani, R.F. de, L. Lorenzi, G.V. Soares, C.A. Figueroa, R.P. Cardoso, T. Belmonte, I.J.R. Baumvol, C.A. Perottoni, J.E. Zorzi, Hardness and wear resistance of the ZrN layer made by plasma nitriding of yttria partially-stabilized zirconia, Ceramica 56 (2010) 300–304.